E2-2001-60

A.P.Bakulev, S.V.Mikhailov, N.G.Stefanis*

QCD-BASED PION DISTRIBUTION AMPLITUDES CONFRONTING EXPERIMENTAL DATA

---

*Institut für Theoretische Physik II, Ruhr Universität, Bochum, Germany

1 Introduction

The pion distribution amplitude (DA) of twist-2, $\varphi_\pi(x, \mu^2)$, i.e., the integral over transverse momenta of the renormalized valence-quark wave function on the light cone, is a gauge- and process-independent characteristic of the pion and, due to factorization theorems [1, 2], it enters as the central input various QCD calculations of hard exclusive processes. A reliable derivation of the pion DA from first principles in QCD is therefore an outstanding problem of paramount importance, given that it contains all of the bound-state dynamics and specifies in a universal way the longitudinal momentum xP distribution of the valence quarks in the pion with momentum P (see, e.g., [3] for a review),

$$\langle 0 \mid \bar{d}(z)\gamma^\mu\gamma_5 u(0) \mid \pi(P)\rangle\big|_{z^2=0} = if_\pi P^\mu \int_0^1 dx e^{ix(zP)} \varphi_\pi(x, \mu^2) . \tag{1}$$

Recently, the CLEO collaboration [4] has measured the $\gamma^*\gamma \to \pi^0$ form factor with high precision. These data sets have been processed by Schmedding and Yakovlev (S&Y) [5] using light-cone QCD sum rules and including perturbative QCD contributions in the NLO approximation (NLA), to obtain useful constraints on the shape of the pion DA in terms of confidence regions for the Gegenbauer coefficients a_2 and a_4. On the other hand, the first direct measurement of the transverse momentum distribution in the pion via diffractive dissociation into di-jets by the Fermilab E791 Collaboration [6], supplemented by new lattice results [7] for the same quantity, also provides the possibility to deduce the shape of the pion DA (modulo inherent method uncertainties).

These important findings inevitably raise the question of whether pion DAs, derived from first principles of QCD, can confront them successfully. The present analysis is a targeted investigation of these issues, the focus being on pion DAs, reconstructed from QCD sum rules with nonlocal condensates (NLC-SR).

This approach, developed in [8, 9, 10, 11] by A. Radyushkin and two of us (A.B. and S.M.) provides a reliable method to construct hadron DAs that inherently accounts for the fact that quarks and gluons can flow through the QCD vacuum with *non-zero momentum* k_q. This means, in particular, that the *average* virtuality of vacuum quarks $\langle k_q^2 \rangle = \lambda_q^2$ is not zero, like in the local sum-rule approach [3], but sizeable. The (vacuum) non-locality parameter is the only one involved in the NLC-SR method, and it has been estimated within the QCD sum-rule approach from the mixed quark-gluon condensate of dimension 5:

$$\lambda_q^2 = \frac{\langle \bar{q}(0)\nabla^2 q(0)\rangle}{\langle \bar{q}(0)q(0)\rangle} \overset{\text{in chiral}}{\underset{\text{limit}}{=}} \frac{\langle \bar{q}(0)\,(ig\,\sigma_{\mu\nu}G^{\mu\nu})\,q(0)\rangle}{2\langle \bar{q}(0)q(0)\rangle} = \begin{cases} 0.4 \pm 0.1 \text{ GeV}^2 & [12] \\ 0.5 \pm 0.05 \text{ GeV}^2 & [13] \end{cases} . \tag{2}$$

Lacking an exact knowledge of NLC of higher dimensionality, the non-locality can only be taken into account in the form of an ansatz.

A simple model is provided by a Gaussian-like behavior of NLC [9, 10], whereas λ_q^{-1} reveals itself as the typical quark-gluon correlation length in the QCD vacuum. Hence, we set in coordinate space, $M_S(z^2) \equiv \langle \bar{q}(0)E(0, z)q(z)\rangle \sim \langle \bar{q}q\rangle \exp\left(-\lambda_q^2|z^2|/8\right),$[†] while the coordinate behavior of other NLCs looks more complicated.

[†]Here, as usual, $E(0, z) = P\exp(i\int_0^z dt_\mu A_\mu^a(t)\tau_a)$ is the Schwinger phase factor required for gauge invariance.

Estimates of λ_q^2 from instanton approaches [14, 15] are somewhat larger: $\lambda_q^2 \approx 2/\rho_c^2 \geq$ 0.6 GeV^2 (where ρ_c is the characteristic size of the instanton fluctuation in the QCD vacuum: $0.33 \leq \rho_c \leq 0.6$ Fm), while lattice calculations [16, 17, 18] confirm qualitatively the Gaussian law for the $M_S(z^2)$ decay, yielding values close to those given in Eq.(2). More calculational details are relegated to [9, 19, 20, 21].

The main results of the present analysis can be summarized as follows. The moments of the pion DA have been re-calculated more accurately and, more importantly, their confidence levels have been determined. In this way, we are able to construct a whole "bunch" (a spectrum) of pion DAs, allowed by the NLC-SR for different values of λ_q^2, as noticed above. The important thing to be emphasized is that the range of this spectrum in the a_2, a_4 plane strongly overlaps with the 95% and also with the 68% region of Schmedding and Yakovlev [5]. Perhaps somewhat surprisingly, the shape of the optimum pion DA, we have determined, is not "dromedary"-like, as the asymptotic solution, but has two maxima (i.e., it is "camel"-like). Nevertheless, we stress, it is not Chernyak–Zhitnitsky (CZ) like either because in the endpoint region it is strongly suppressed.

2   Spectrum of pion DAs from NLC-SR

Revision of pion DA moments. The NLC-SR for the DAs of the pion and the effective $A_1 + \pi'$-resonance, $\varphi_\pi(x)$ and $\varphi_{A_1}(x)$, respectively, which appear in the "axial" channel, were constructed in [8, 9] and were analyzed in [9, 20]. Here we display only the sum rule itself:

$$
(f_\pi)^2 \, \varphi_\pi(x) + (f_{A_1})^2 \, \varphi_{A_1}(x) e^{-m_{A_1}^2/M^2} = \int_0^{s_0^A} \rho^{pert}(x; s) e^{-s/M^2} ds + \Delta\Phi_S(x; M^2) \quad (3)
$$
$$
+ \Delta\Phi_V(x; M^2) + \Delta\Phi_{T_1}(x; M^2) + \Delta\Phi_{T_2}(x; M^2) + \Delta\Phi_{T_3}(x; M^2) + \Delta\Phi_G(x; M^2)
$$

and re-estimate the moments and their error bars. The NLC contributions encoded in $\Delta\Phi_\Gamma(x; M^2)$ on the rhs of the SR, as well as the explanation of the individual terms are discussed in [9, 20]. The corrected form of the contribution for $\Delta\Phi_{T_1}(x; M^2)$ (originating from the NLC $\langle \bar{q}Gq \rangle$) and also the main contribution to the rhs of the SR, which is accumulated in the $\Delta\Phi_S(x; M^2)$ term (owing to the NLC M_S), are shown in Appendix A.

Both the sensitivity and the stability of the NLC-SR are considerably improved relative to the standard SR (but nevertheless we still assume a rather conservative size of the errors of the order of 10%). This allows us to determine the first ten moments $\langle \xi^N \rangle_\pi \equiv \int_0^1 \varphi_\pi(x)(2x - 1)^N dx$ of the pion DA quite accurately. This is illustrated in Fig. 1(a), where the curves for $\langle \xi^4 \rangle_\pi$ are represented as functions of the Borel parameter M^2 plotted within the range of the stability window of the SR. The solid line (optimum moment) is determined from the NLC-SR (3), for $s_0 = 2.2$ GeV^2, while the broken lines give the results for thresholds varied by 10% around this value, which turns out to be practically independent of the moment order N [9, 20]. Then, the fidelity windows are: 0.5 GeV$^2 \leq M^2 \leq 2.0$ GeV^2 for all $N = 0, 2, \ldots, 10$. Notice that the range of stability and the Borel fidelity windows almost coincide with each other, starting for all N at $M^2 \approx 0.6$ GeV^2.

2

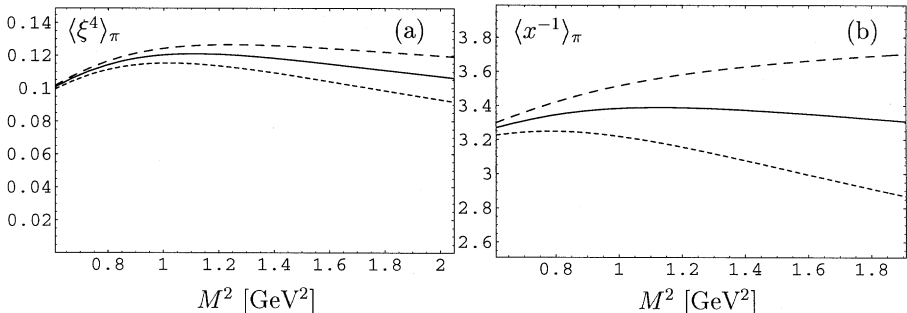Fig. 1: (a) Original SR for the moment $\langle\xi^4\rangle_\pi$ and (b) "daughter SR" for the inverse moment $\langle x^{-1}\rangle_\pi^{\text{SR}}$, both as functions of the Borel parameter M^2, as obtained from the NLC-SRs. Both kinds of SRs were processed by including the A_1-meson with $s_0 = 2.2$ GeV^2. For the depicted range of M^2, the fidelity and stability windows almost coincide. Solid lines correspond to the optimal threshold s_0, whereas broken lines denote the results for the upper (long-dashed line) and lower (short-dashed line) moment limit with a 10%-variation of s_0.

Type of SR	f_M (GeV)	$N = 2$	$N = 4$	$N = 6$	$N = 8$	$N = 10$	$\langle x^{-1}\rangle$
Asympt. DA		0.2	0.086	0.047	0.030	0.021	3
NLC SR [9] : π	0.131	0.25	0.12	0.07	–	–	–
NLC SR [20] : π	0.131(2)	0.25(1)	0.110(7)	0.054(3)	0.031(2)	0.0217(7)	2.75(5)
NLC here : π	0.131(8)	0.265(20)	0.115(12)	0.061(8)	0.037(5)	0.024(4)	3.35(32)
NLC here : $A_1\&\pi'$	0.210(17)	0.21(2)	0.116(12)	0.078(8)	0.055(6)	0.042(5)	3.6(4)
CZ SR [22, 3] : π	0.131	0.40	0.24	–	–	–	–

Table 1. The moments $\langle\xi^N\rangle_M(\mu^2)$ determined at $\mu^2 \sim 1$ GeV^2 with associated errors put in parentheses. Recall that CZ give all moments normalized at the lower scale $\mu_0^2 = 0.5$ GeV^2.

The important convolution $\langle x^{-1}\rangle_\pi = \int_0^1 \frac{\varphi_\pi(x)}{x} dx$, appears in the perturbative calculation of the $\gamma^*\gamma \to \pi^0$ process. We construct a "daughter SR" directly for this quantity from Eq. (3) by integrating its rhs with the weight $1/x$. Due to the smooth behavior of the NLC at the end points $x = 0, 1$, this integral is well defined, supplying us with an independent SR, with a rather good stability behavior of $\langle x^{-1}\rangle_\pi^{\text{SR}}(M^2)$, as one sees from Fig. 1(b). To understand this behavior, let us recall an important feature of the NLC, encoded in $\Delta\Phi_\Gamma(x; M^2)$. This contribution is suppressed in the vicinity of the end-points $x = 0, 1$, the range of suppression being controlled by the value of the non-locality para-

meter λ_q^2. The larger this parameter, at fixed resolution scale $M^2 > \lambda_q^2$, the stronger the suppression of the NLC contribution. Similarly, an excess of the value of $\langle x^{-1}\rangle_\pi$ over 3 (asymptotic DA) is also controlled by the value of λ_q^2, becoming smaller with increasing λ_q^2. Note, that instanton-based models demonstrate the same behavior of the DA with a non-locality parameter proportional to ρ_c^{-2} [23].

From Table 1 one infers that the mean values of the re-calculated moments are close to the old ones, whereas the value of $\langle x^{-1}\rangle_\pi^{\rm SR}$ changes significantly. The reason is the corrected term $\Delta\Phi_{T_1}(x; M^2)$ (in the NLC-SR), which allows us now to reconcile this quantity with the value obtained by calculating it with the model DAs (see below). The new estimates of the error bars in Table 1 have been formed from different sources. Note that the most significant error (about 50%) stems from the uncertainties of the parameters of the $A_1 + \pi'$-resonance.

Spectrum of admissible pion DAs. Models for the pion DA, in correspondence to the moments in Table 1, can be constructed in different ways [9, 20]. However, it appears that two-parameter models, the parameters being the Gegenbauer coefficients a_2 and a_4 (as also used in [5]), enable one to fit all the moment constraints for $\langle \xi^N\rangle_\pi$ given in the Table, as well as to reproduce the value of $\langle x^{-1}\rangle_\pi$ within the quoted error range.[‡] The optimum model DA is

$$\varphi_1^{\rm opt}(x) = \varphi^{\rm as}(x)\left[1 + a_2^{\rm opt1}\cdot C_2^{3/2}(2x-1) + a_4^{\rm opt1}\cdot C_4^{3/2}(2x-1)\right] , \qquad (4)$$

$$a_2^{\rm opt1} = +0.188 , \quad a_4^{\rm opt1} = -0.130 , \quad \text{with } \chi^2 \approx 10^{-3} , \qquad (5)$$

yielding $\langle x^{-1}\rangle_1^{\rm opt} = 3.174$. But one can construct a whole admissible set (a spectrum), $\{\varphi_1(x; a_2, a_4)\}$, of such models by demanding that the associated moments lie inside the error bars, presented in Table 1. This set of DAs approximately corresponds to those parameters (a_2, a_4), which satisfy $\chi^2 \leq 1$. In this way, we obtain a "bunch" of admissible DA profiles, shown in Fig. 2(a) in terms of dashed lines, in addition to the optimum one (thick solid line). For these DAs, the corresponding values of $\langle x^{-1}\rangle_{\varphi_1}$ vary in the interval

$$3.08 \leq \langle x^{-1}\rangle_{\varphi_1} \leq 3.24 \quad \text{vs} \quad 3.03 \leq \langle x^{-1}\rangle_{\pi 1}^{SR} \leq 3.67 . \qquad (6)$$

Let us mention at this point that in the standard approach the value of $\langle x^{-1}\rangle(\mu^2)$ cannot be determined from the *sum rule itself* due to the presence of singular $\delta(x)$-terms. On the other hand, for the CZ *model* DA, one finds $\langle x^{-1}\rangle_{\rm CZ}(\mu^2) \approx 5.1$ at normalization scale $\mu^2 \approx (0.7)^2$ GeV^2 or ≈ 4.44 at the scale $\mu^2 \approx 1$ GeV^2.

The above results have been obtained within the framework of NLCs, employing a single non-locality parameter, viz., λ_q^2, fixed at the so-called "standard" value of 0.4 GeV^2 [12]. To examine the role of this parameter in determining the structure of the model DAs, we constructed another set of amplitudes, $\varphi_2(x)$, fixing it at the higher, yet admissible, value $\lambda_q^2 = 0.5$ GeV^2 [13]. Again, an "optimum" DA, $\varphi_2^{\rm opt}(x)$, was determined with coefficients $a_2^{\rm opt2} = +0.126$, $a_4^{\rm opt2} = -0.091$ with a profile similar to that of $\varphi_1^{\rm opt}(x)$, as Fig. 2(b) reveals. Note, however, that now the envelope of the "bunch" becomes quite close to the asymptotic DA, i.e., "dromedary-like (convex) at $x = 1/2$ and correspondingly

---

[‡]Note that SY *assume* that $a_{n>4}$ are small, while in our approach these coefficients have been *calculated* up to $N = 10$ and found to be numerically negligible.
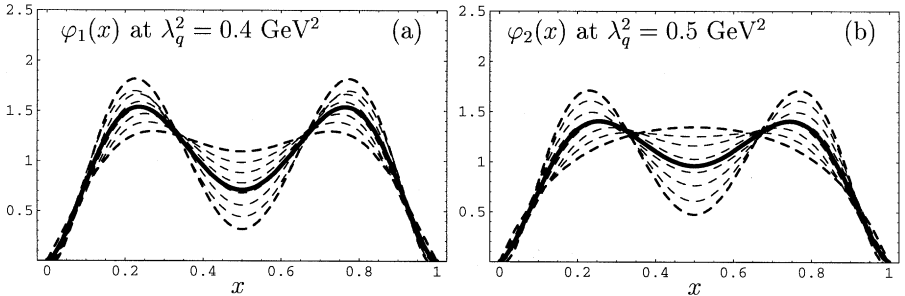
Fig. 2: Graphical representation of $\varphi_1(x)$ (part (a)) and $\varphi_2(x)$ (part (b)). The thick solid lines in both plots denote $\varphi_{1,2}^{\mathrm{opt}}(x)$, i.e., the best fit to the determined values of the moments (see Table 1), whereas dashed lines illustrate admissible options with $\chi^2 \leq 1$.

it exhibits less suppression in the endpoint region $x = 0, 1$. We note in passing that a suppression of the endpoint region as strong as possible (for a discussion we refer to [24]) is important in order to improve the self-consistency of perturbative QCD in convoluting the pion DA with the specific hard-scattering amplitude of particular exclusive processes. As before, the values of the inverse moment $\langle x^{-1} \rangle_{\pi2}^{\mathrm{SR}}$, extracted from the new SR, and those following from the model $\varphi_2(x)$, are mutually consistent:

$$3.05 \leq \langle x^{-1} \rangle_{\varphi_2} \leq 3.22 \quad \mathrm{vs} \quad 2.87 \leq \langle x^{-1} \rangle_{\pi2}^{\mathrm{SR}} \leq 3.51 . \tag{7}$$

It is worth remarking here that this "camel-like" structure of the "best fit" (alias, the optimum) DAs for both considered values of the non-locality parameter λ_q^2, displayed in Fig. 2(a,b) can actually be traced back to a definite origin. Crudely speaking, this shape structure is the net result of the interplay between the perturbative contribution and the non-perturbative term $\Delta\Phi_S(x)$ that dominates the rhs of the SR in Eq. (3). The fact that the function $\Delta\Phi_S(x)$ is not singular in x and has a dip at the central point of the interval $[0, 1]$ is also reflected in the shapes of the DAs.

3 QCD SR results vs CLEO data

Overlap of regions in a_2, a_4 plane. Let us now draw in Fig. 3(a) the regions of admissible pairs (a_2, a_4), determined in correspondence with the error bars of the moments, in order to compare them with the experimental constraints supplied by the recent high-precision CLEO data [4]. The latter are processed in the plot in Fig. 3(b) in the form of confidence regions, extracted by Schmedding and Yakovlev [5] using a NLO light-cone QCD SR analysis that (approximately) corresponds to an average normalization point of $\mu = 2.4$ GeV.

The region, corresponding to the bunch of DAs, determined at the "standard" value $\lambda_q^2 = 0.4$ GeV^2, and evolved to $\mu = 2.4$ GeV in Fig. 2(a), is enclosed in Fig. 3(a) by a slanted rectangular area. Superimposing this area with the "ellipses" pertaining to a 68% (solid line) and a 95% (dashed line) confidence region, [5], we show in Fig. 3(b) to which extent our estimates for the pion DAs agree with the CLEO data. In particular,
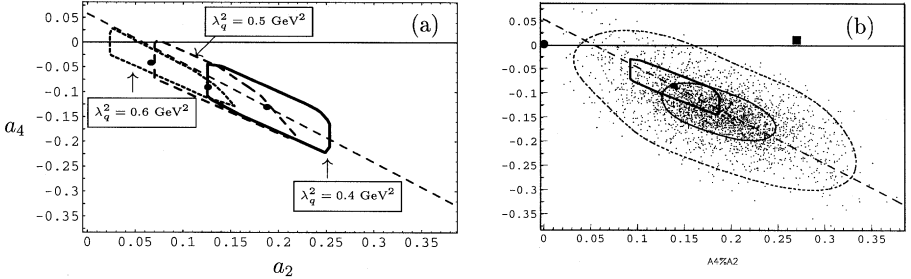
5

Fig. 3: (a) The parameter space of (a_2, a_4) pairs (enclosed by a thick solid line), corresponding to the allowed values of the second and fourth Gegenbauer coefficients, calculated within the NLC-SR approach for three different values of λ_q^2 at $\mu = 1$ GeV. The optimum DA is denoted by a black dot. (b) shows how our estimate of the confidence region with $\lambda_q^2 = 0.4$ GeV^2 at $\mu = 2.4$ GeV overlaps with those displayed in Fig. 6 of Ref.[5]. Bold dots in plot (b) mark the parameter pairs for the asymptotic (big black dot), Chernyak-Zhitnitsky (full square) and our optimum (with respect to the SR) DA (black dot). Contour lines show 68% (solid line) and 95% (dashed line) confidential regions, extracted by Schmedding and Yakovlev from 3000 randomly chosen sets of CLEO data [4]. The small axis of the "ellipses" is generated by experimental-statistical uncertainties, whereas the large one results from theoretical-systematical uncertainties.

the central point $(\bar{a}_2^{\mathrm{opt}}, \bar{a}_4^{\mathrm{opt}})$ of the slanted rectangle lies just the 68%-region and the lower corner of it "touches" the central point (a_2^*, a_4^*) of the SY plot:

$$a_2^* = 0.190, \qquad a_4^* = -0.14 , \tag{8}$$

$$\bar{a}_2^{\mathrm{opt1}} = 0.139, \qquad \bar{a}_4^{\mathrm{opt1}} = -0.082 . \tag{9}$$

Given the errors determined by SY,

$$a_2 = a_2^* \pm 0.04(\mathrm{stat}) \pm 0.09(\mathrm{syst}), \quad a_4 = a_4^* \pm 0.03(\mathrm{stat}) \mp 0.09(\mathrm{syst}) , \tag{10}$$

one realizes that our theoretical estimates are quite compatible with their experimental constraints. The region enclosed by the slanted rectangle bounded by the long-dashed line along the "diagonal" (see below) in Fig. 3(a), corresponds to the bunch of DAs displayed in Fig. 2(b). Though still within the 95% confidence region of SY, it is, however, mostly outside the central 68% region. Finally, the third slanted rectangle limited by the short-dashed contour, and shifted along the "diagonal" to the upper left corner of the figure in Fig. 3(a), corresponds to a *trial* NLC-DA with $\lambda_q^2 = 0.6$ GeV^2. This value falls actually outside the standard QCD NLC-SR bounds in Eq. (2) for λ_q^2. Remarkably, the image of this region in Fig. 3(b) (not displayed) would lie completely outside the central region as a whole. Therefore, we conclude that the CLEO data does not prefer the value $\lambda_q^2 = 0.6$ GeV^2, in full agreement with previous QCD SR estimates.[§]

[§] A very interesting detail in Fig. 3(a) is that the intersection set of all three admissible regions represented by the slanted rectangles is located around (and contains) the optimum point for the value $\lambda_q^2 = 0.5$ GeV^2, though its image in Fig. 3(b) lies outside, but close to the upper boundary of the 68% SY region.

Role of the "diagonal". By measuring the $\gamma + \gamma^* \to \pi$ form factor, $F_{\gamma\gamma^*\pi}$, one mainly probes the pion inverse moment $\langle x^{-1} \rangle_\pi = 3(1 + a_2 + a_4 + \ldots)$. To illustrate this, let us apply the leading twist NLA expression [25] to the $Q^2 F_{\gamma\gamma^*\pi}$,

$$\frac{3}{4\pi} Q^2 \left(F_{\gamma\gamma^*\pi} \approx C \otimes \varphi_\pi \right) = I = 3 \left[1 + a_2 + a_4 + \ldots + \alpha_s (\Delta_0 + a_2 \Delta_2 + a_4 \Delta_4 + \ldots) \right] . \tag{11}$$

Here C is a coefficient function in the factorized amplitude for the process at NLO; Δ_n gives the size of the leading radiative corrections to the contribution of the Nth Gegenbauer eigenfunction entering the expansion of $\varphi_\pi(x)$. It should be noted that this standard factorization formula is not well established when one of the photons in the process is on-shell. Nevertheless, for demonstration purposes this approach is good enough. The correspondence

$$I(\mu^2) = \langle x^{-1} \rangle_\pi(\mu^2) + 3\alpha_s(\mu^2)\Delta_0 \tag{12}$$

is slightly smeared by radiative corrections due to higher eigenfunctions in Eq. (11). Therefore, constraints imposed by $F_{\gamma\gamma^*\pi}$ measurements are in reality constraints for the combination $a_2 + a_4 + \ldots$, modulo contributions from radiative corrections and higher twists. Due to this reason, the admissible region for the desired points (a_2, a_4) in [5], (Fig. 3(b)), is, so to speak, stretched along a "diagonal" defined by $a_2 + a_4 = \text{const}$. The value of this constant can be easily extracted from the data with a reasonable accuracy,[¶] using Eqs. (9), (10), to obtain

$$a_2 + a_4 = 0.05 \pm 0.07 \tag{13}$$

(large systematic errors cancel!) that should be compared with our value

$$\bar{a}_2 + \bar{a}_4 = 0.056 \pm 0.033 . \tag{14}$$

Hence, we see that an "experimental" quantity (Eq. (13)) expressively agrees with those obtained in the NLC-SR (cf. Eq. (14)). On the other hand, the direct estimate for $\langle x^{-1} \rangle_\pi$ from this SR (at $\mu^2 \sim 1$ GeV^2 in Table 1) is also in agreement with both of these estimates, $\langle x^{-1} \rangle_\pi / 3 - 1 \approx 0.1 \pm 0.1$. The evolution of this quantity to the scale $\mu^2 = (2.4 \text{ GeV})^2$ should eventually make the agreement more pronounced. To complete these considerations, let us mention that the empirical SY estimate, introduced in [5] for a "deformed diagonal" in the (a_2, a_4)-plane

$$a_2 + 0.6 a_4 = 0.11 \pm 0.03 , \tag{15}$$

is also satisfied by the values of the central point of our admissible region, namely,

$$\bar{a}_2 + 0.6 \bar{a}_4 = 0.09 \pm 0.039 . \tag{16}$$

We emphasize that the radiative corrections in Eqs. (11), (12) are particularly important because it turns out that they dominate over the "non-perturbative" a_2, a_4 contribution. To make this point more apparent, let us consider the asymptotic DA

[¶]At the same time, the theoretical-systematical errors to every pair of values of a_2, a_4 appear to be very large, see Eq. (10).

in NLO approximation [26] (see Eqs. (B.2), (B.3) in Appendix B). Then, we find that this eigenfunction supplies the main contribution to I and $\alpha_s\Delta_0$:

$$\alpha_s\Delta_0 = \frac{\alpha_s(\mu^2)}{4\pi}\left[-5C_F + \left(2C_F - \frac{b_0}{3}\right)\right] = -7\,\frac{\alpha_s(\mu^2)}{4\pi} \approx -0.17\;. \qquad (17)$$

The first contribution, $-5C_F$, originates from the coefficient function (see [27]), while the second one, $(2C_F - b_0/3)$, from the modification of the asymptotic DA at NLO [26]. The final estimate, -0.17, corresponds to the value $\alpha_s/(4\pi) = 0.024$ [28] at the normalization point $\mu = 2.4$ GeV. We see that the estimate for $\alpha_s\Delta_0$ is indeed 3 times larger than those for $a_2 + a_4$, considered above, and for that reason it controls the level of accuracy in the determination of the latter.[||] The twist-4 contribution to the form factor is also important (see [5]), being of the same order as $a_2 + a_4$ but having the opposite sign. The overall radiative correction to the contribution of still higher eigenfunctions is also negative and small in comparison to the estimate in Eq. (17),

$$\frac{\alpha_s(\mu^2)}{4\pi}\cdot(a_2\Delta_2 + a_4\Delta_4) \approx 0.024\cdot(-0.58) = -0.014\;.$$

To further improve the theoretical accuracy of extracting a_2 and a_4 (from experimental data), one should first obtain an estimate for $C \otimes \varphi_{\mathrm{as}}$ in next to NLO approximation because this contribution will certainly dominate in that order.

4 Comparison with results from different sources.

In this section we compare the results of our analysis with new evidences for the form of the pion DA, following from hadron phenomenology, lattice simulations and instanton-based models. However, keep in mind that the information provided from these sources bears uncertainties the size of which is difficult to estimate.

DA from π^- into di-jets via diffractive dissociation. It is tempting to compare the results obtained and discussed above with the intriguing interpretation of experimental data on di-jet production in pion-nucleon interactions [6]. This process was suggested already in [31] as a tool to measure the shape of the pion DA directly from the data via diffractive dissociation into two jets. Such an experiment was carried out very recently by the Fermilab E791 Collaboration [6] by measuring the transverse momentum distribution of the diffractive di-jets in two windows of k_t: $1.25 \le k_t \le 1.5$ GeV and $1.5 \le k_t \le 2.5$ GeV . We have found that their experimental deduction for the shape of the pion DA in the lower window can be well approximated by a model with two Gegenbauer coefficients to read

$$\varphi_\pi^{\mathrm{fit}}(x,Q^2) = \varphi^{\mathrm{as}}(x)\left[1 + a_2^{\mathrm{fit}}(Q^2)\cdot C_2^{3/2}(2x-1) + a_4^{\mathrm{fit}}(Q^2)\cdot C_4^{3/2}(2x-1)\right]\;, \qquad (18)$$

[||]An analysis in leading approximation, performed in [29] for the phenomenological value $I \approx 2.4$, leads to the conclusion that $I \approx \langle x^{-1}\rangle_\pi$, so that the associated DA is forced to be narrower than the asymptotic one. But in NLO this estimate transforms into Eqs. (11), (12) and therefore one can conclude that the value of $\langle x^{-1}\rangle_\pi$ is larger than 3, with the pion DA being broader than the asymptotic one. Indeed, Fig. 3(b) demonstrates exactly this fact in detail. In the same context we mention that a narrower DA than the asymptotic one was also used in the calculation of $F_{\pi\gamma}$ in [30] yielding a prediction somewhat below the CLEO data and leading to the suggestion that the shape of the "true" pion DA must be broader than that of the asymptotic one.

with $\chi^2 \approx 10^{-2}$ and $a_2^{\text{fit}} = 0.121$, $a_4^{\text{fit}} = 0.012$ at $Q^2 \approx 8$ GeV^2. Despite the large "diagonal" value $a_2^{\text{fit}}(\mu^2) + a_4^{\text{fit}}(\mu^2) \approx 0.143$ (at $\mu = 2.4$ GeV), resulting from this model, it is still consistent with the SY constraints, as one realizes by comparing it with the values given in Eqs. (13), (14). The symbol "star", associated with $\varphi_\pi^{\text{fit}}(\mu^2)$, is located in Fig. 4(b) on the upper boundary of the SY 95% region and above the diagonal. Fig. 4(a) shows the profile of the E791-fit (thick solid line) in comparison with our "optimum" DAs for $\lambda_q^2 = 0.4$ (dashed line) and $\lambda_q^2 = 0.5$ GeV^2 (solid line), both evolved to $Q^2 \approx 8$ GeV^2. Taking into account that the accuracy of the data is not better then 10%, one is tempted to conclude that the DA shape from the di-jet data is in fact not far away from the φ_2-bunch. Note that the authors of the second paper in [31] have discussed this treatment of di-jet production data and concluded that the interpretation of them with respect to the pion DA is yet questionable. Indeed, inspection of their Fig. 3 [6] reveals that the results (data) for $x < 0.1$ and $x > 0.85 - 0.9$ are different, exhibiting the limitations of the accuracy of their fit in the endpoint regions.
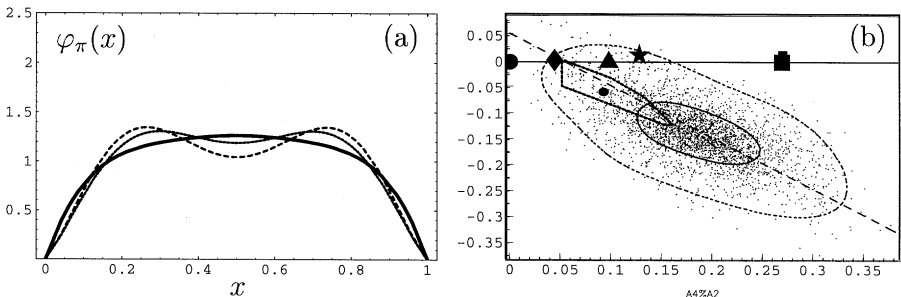

Fig. 4: (a) Selected profiles of $\varphi_\pi(x, \mu^2 = 8$ GeV$^2)$. The short (long) dashed line corresponds to our "optimum" DA model, $\varphi_1^{\text{opt}}(x)$ at $\lambda_q^2 = 0.4$ GeV^2 ($\varphi_2^{\text{opt}}(x)$ at 0.5 GeV^2) and the solid line to the fit to the model deduced from the experimental data on di-jet production in pion-nucleon interactions [6]. (b) This plot is obtained by inserting into Fig. 6 of Ref.[5] the confidence region determined for the φ_2-bunch (at $\lambda_q^2 = 0.5$ GeV^2) and confined in the slanted rectangle. The E791 Collaboration fit[6], Eq. (18), is denoted by a black star, whereas the Dalley model, Eq. (19), is marked by a black triangle. All model DAs shown are evolved to $\mu = 2.4$ GeV.

Transverse lattice. Quite recently, Dalley [7] has used the data points in a transverse-lattice calculation to deduce the shape of the pion DA and approximated it by the following analytic form

$$\varphi^{\text{lat}}(x, \mu_0^2) = \varphi^{\text{as}}(x) \left[1 + 0.133 \cdot C_2^{3/2}(2x - 1) \right] \tag{19}$$

at $\mu_0^2 \sim 1$ GeV^2. The shape parameters a_2, a_4 of this DA are inside the admissible 95% region in Fig. 4(b) (black triangle) and somewhat closer to the diagonal than the fit of E791. Because of several approximations in this calculation, the quality of the deduced fit is unknown and as a result the errors in the coefficients are presumably large. Hence, we may regard this model DA as being only qualitatively consistent with the φ_2-bunch.

Two things are worth to be remarked. First, this new model fit is in conflict with the

DA shape predicted in [32] and more recently in [33] using the same Hamiltonian and Fock space truncation, but employing continuous basis functions rather than the discrete light-cone quantization applied by Dalley. Second, if the shape obtained is very close to the asymptotic one, then it is again ruled out by the CLEO data, as its outside the SY confidence regions. For the sake of completeness, we mention in this context that other lattice attempts [34, 35] yield unrealistically small values of the moment $\langle \xi^2 \rangle_\pi$.

Instanton-induced models. Instanton-induced models, worked out in [36, 37], usually lead to DA shapes close to the asymptotic one. As a consequence, such DAs are definitely ruled out by the SY constraints shown in Fig. 4(b). However, these DAs satisfy "a softer constraint", also derived by SY in [5] (see Fig. 7 there). In fact, the confidence regions derived this way, are somewhat enlarged with the effect that the asymptotic DA is just "inside" the larger region and positioned at the upper end of the diagonal. Note that instanton-induced models prefer a higher value of the vacuum quark virtuality: $\lambda_q^2 \geq 0.6$ GeV^2. For such a value of the parameter λ_q^2 (unrealistically large for QCD SRs), the condensate contribution on the rhs of Eq. (3) becomes small in comparison to the perturbative one. As a consequence of this, the corresponding DA appears to be closer to the asymptotic one, as we have already indicated (cf. Fig. 3(a), where one sees that the center of the slanted rectangle for this λ_q^2 value is much closer to the a_4 axis and hence to the asymptotic DA.)

A separate case of an instanton-induced pion DA, consistent with the SY constraints, has been derived by Praszalowicz [38]. We included this model in Fig. 4(b) by the label "full diamond".

5 Conclusions

1. We performed an accurate analysis of QCD SR with NLCs for the pion DA and obtained admissible sets of them with respect to the SR constraints for different values of the non-locality parameter λ_q^2. Confronting these determined DA spectra with the constraints obtained by SY in [5] from the high-precision CLEO experimental data [4], we showed that they satisfy them *quantitatively* (cf. Fig. 3 and Fig. 4(b)).

2. We found that the predictions for the profile of the pion DA deduced from the di-jet production (E791 Collaboration) [6] and those extracted from the simulation on a transverse lattice [7] are consistent only with the 95% SY constraints (2σ-deviation criterium), but not with the 68% SY constraints (1σ-deviation criterium). Moreover, they are located near the boundary of the 2σ-region obtained with the standard error estimation. As shown in Fig. 4(b), the di-jet prediction is not too far from the φ_2-bunch region (with $\lambda_q^2 = 0.5$ GeV^2), though a quantitative comparison calls for a higher accuracy of the data processing. On the other hand, the lattice result qualitatively also agrees with the set of our DAs (the φ_2-bunch) (see Fig. 4(b)), but a more detailed comparison is obscured by the unknown quality of this method.

3. The existing predictions from instanton-induced models are too close to the asymptotic DA and therefore they are only consistent with the "softened" version of the SY constraints (see for details in [5]), except for the new model by Praszalowicz [38], which is just outside the confidence region of the φ_2-bunch and on the boundary of the 95%-region

of SY.

A   Expressions for nonlocal contributions to SR

The form of contributions of NLCs to the OPE on the rhs of Eq. (3) depends on the modelling of NLCs. At the same time, the final results of the evaluation of the SRs show stability against variations of this modelling, provided the scale of the average vacuum quark virtuality λ_q^2 is fixed. Here, we used the model (delta-ansatz) suggested in [9, 10] and used extensively in [20, 21]. This model leads to a Gaussian decay of the scalar quark condensate $M_S(z^2)$. For the four-quark condensate, the factorization ansatz is applied to reduce its contribution to a pair of scalar condensates. In the NLC approach this may lead to an overestimate of the four-quark condensate contribution, $\Delta\Phi_S(x; M^2)$, because it evidently neglects the correlation between these pairs. Below, $\Delta \equiv \lambda_q^2/(2M^2)$, $\bar{\Delta} \equiv 1 - \Delta$:

$$\Delta\Phi_S\left(x; M^2\right) = \frac{A_S}{M^4}\frac{18}{\bar{\Delta}\Delta^2}\Big\{\theta\left(\bar{x} > \Delta > x\right)\bar{x}\left[x + (\Delta - x)\ln\left(\bar{x}\right)\right] + (\bar{x} \to x) +$$
$$+\theta(1 > \Delta)\theta\left(\Delta > x > \bar{\Delta}\right)\left[\bar{\Delta} + (\Delta - 2\bar{x}x)\ln(\Delta)\right]\Big\} \text{ (A.1)}$$

Instead of (A.5) in [20], we have

$$\Delta\Phi_{T_1}\left(x; M^2\right) = -\frac{3A_S}{M^4}\theta(1 > 2\Delta)\left\{[\delta(x - 2\Delta) - \delta(x - \Delta)]\left(\frac{1}{\Delta} - 2\right) + \theta(2\Delta > x)\cdot\right.$$
$$\left.\theta(x > \Delta)\frac{\bar{x}}{\bar{\Delta}}\left[\frac{x - 2\Delta}{\Delta\bar{\Delta}}\right]\right\} + (\bar{x} \to x) \ . \tag{A.2}$$

Here, $A_S = (8\pi/81)\langle\sqrt{\alpha_s}\bar{q}(0)q(0)\rangle^2$, whereas for the quark and gluon condensates we use the standard estimates $\langle\sqrt{\alpha_s}\bar{q}(0)q(0)\rangle \approx (-0.238 \text{ GeV})^3$, $\langle\alpha_s GG\rangle/12\pi \approx 0.001 \text{ GeV}^4$ [39].

B   Radiative corrections

The radiative corrections to the correlator and to the pion DA are

$$\rho^{\text{pert}}(x, s) = \frac{3x\bar{x}}{2\pi^2}\left\{1 + a_s\left[C_F\left(2 - \frac{\pi^2}{3} + \ln^2(\bar{x}/x)\right) + C_F\left(2\ln\left(s/\mu^2\right) + 3\right)\right]\right\}\text{(B.1)}$$

$$\varphi_{\text{as}}^{\text{NLA}}(x) = 6x\bar{x}\left\{1 + a_s\left[C_F\left(2 - \frac{\pi^2}{3} + \ln^2(\bar{x}/x)\right) + b_0\left(\ln(x\bar{x}) + \frac{5}{3}\right)\right]\right\} \ , \tag{B.2}$$

$$\langle x^{-1}\rangle_{\text{as}} = 3\left[1 + a_s\left(2C_F - \frac{1}{3}b_0\right)\right] \ . \tag{B.3}$$

11

Here, b_0 is the first β-function coefficient, $b_0 = (11/3)C_A - (4/3)TrN_f$; $a_s = \alpha_s(\mu^2)/4\pi$, $\Lambda_{(3)}^{\mathrm{NLO}} \approx 0.465$ GeV, $\alpha_s^{\mathrm{NLO}}(m_\tau^2) \approx 0.358$, see, e.g., [28]. We perform a 2-loop evolution of the pion DA following the approach presented in the first paper in [25] and using the so-called "optimized MS-scheme" [40].

References

[1] V. L. Chernyak and A. R. Zhitnitsky, JETP Lett. 25 (1977) 510.

[2] G. P. Lepage and S. J. Brodsky, Phys. Lett. B 87 (1979) 359; Phys. Rev. D 22 (1980) 2157;
A. V. Efremov and A. V. Radyushkin, Theor. Math. Phys. 42 (1980) 97; Phys. Lett. B 94 (1980) 245.

[3] V. L. Chernyak and A. R. Zhitnitsky, Phys. Rept. 112 (1984) 173.

[4] J. Gronberg et al. (CLEO Collaboration), Phys. Rev. D 57 (1998) 33.

[5] A. Schmedding and O. Yakovlev, Phys. Rev. D 62 (2000) 116002.

[6] E. M. Aitala et al. (Fermilab E791 Collaboration), hep-ex/0010043;
D. Ashery, hep-ex/9910024; Nucl. Phys. Proc. Suppl. B 90 (2000) 67.

[7] S. Dalley, hep-ph/0101318.

[8] S. V. Mikhailov and A. V. Radyushkin, JETP Lett. 43 (1986) 712.

[9] S. V. Mikhailov and A. V. Radyushkin, Sov. J. Nucl. Phys. 49 (1989) 494; Phys. Rev. D 45 (1992) 1754.

[10] A. P. Bakulev and A. V. Radyushkin, Phys. Lett. B 271 (1991) 223.

[11] S. V. Mikhailov, Phys. Atom. Nucl. 56 (1993) 650.

[12] V. M. Belyaev and B. L. Ioffe, Sov. Phys. JETP 57 (1983) 716;
A. A. Ovchinnikov and A. A. Pivovarov, Sov. J. Nucl. Phys. 48 (1988) 721.

[13] A. A. Pivovarov, Bull. Lebedev Phys. Inst. 5 (1991) 1.

[14] M. V. Polyakov and C. Weiss, Phys. Lett. B 387 (1996) 841.

[15] A. E. Dorokhov, S. V. Esaibegian, and S. V. Mikhailov, Phys. Rev. D 56 (1997) 4062.

[16] M. D'Elia, A. Di Giacomo, and E. Meggiolaro, Phys. Rev. D 59 (1999) 054503.

[17] E. Meggiolaro, Nucl. Phys. Proc. Suppl. 83 (2000) 512.

[18] H. G. Dosch et al., JHEP 07 (2000) 023.

[19] A. P. Bakulev and S. V. Mikhailov, Z. Phys. C 68 (1995) 451; Mod. Phys. Lett. A 11 (1996) 1611.

[20] A. P. Bakulev and S. V. Mikhailov, Phys. Lett. B 436 (1998) 351.

[21] A. P. Bakulev and S. V. Mikhailov, Eur. Phys. J. C (2001) to be published (DOI 10.1007/s100520100603) [hep-ph/0006206].

[22] V. L. Chernyak and A. R. Zhitnitsky, Nucl. Phys. B 201 (1982) 492; ibid. B 214 (1983) 547(E).

[23] I. V. Anikin, A. E. Dorokhov, and Lauro Tomio, Phys. Lett. B 475 (2000) 361.

[24] N. G. Stefanis, W. Schroers, and H.-Ch. Kim, Phys. Lett. B 449 (1999) 299.

[25] E. P. Kadantseva, S. V. Mikhailov, and A. V. Radyushkin, Sov. J. Nucl. Phys. 44 (1986) 326;
E. Braaten, Phys. Rev. D 28 (1983) 524.

[26] D. Müller, Phys. Rev. D 49 (1994) 2525; Phys. Rev. D 51 (1995) 3855.

[27] I. V. Musatov and A. V. Radyushkin, Phys. Rev. D 56 (1997) 2713.

[28] A. A. Pivovarov, Z. Phys. C 53 (1992) 461;
F. Le Diberder and A. Pich, Phys. Lett. B 286 (1992) 147.

[29] A. V. Radyushkin and R. T. Ruskov, Nucl. Phys. B 481 (1996) 625.

[30] N. G. Stefanis, W. Schroers, and H.-Ch. Kim, Eur. J. Phys. C 18 (2000) 137.

[31] L. Frankfurt, G. A. Miller, and M. Strikman, Phys. Lett. B 304 (1993) 1; Found. Phys. 30 (2000) 533.

[32] M. Burkardt and H. El-Khozondar, Phys. Rev. D 60 (1999) 054504.

[33] M. Burkardt and S. Seal, hep-ph/0101338.

[34] D. Daniel, R. Gupta, and D. G. Richards, Phys. Rev. D 43 (1991) 3715.

[35] L. Del Debbio et al., Nucl. Phys. Proc. Suppl. 83 (2000) 235.

[36] V. Yu. Petrov et al., Phys. Rev. D 59 (1999) 114018.

[37] I. V. Anikin, A. E. Dorokhov, and L. Tomio, Phys. Part. Nucl. 31 (2000) 509.

[38] M. Praszałowicz and A. Rostworowski, Cracow preprint TPJU-4/2001.

[39] M. A. Shifman, A. I. Vainshtein, and V. I. Zakharov, Nucl. Phys. B 147 (1979) 385; 448; 519.

[40] A. P. Bakulev, A. V. Radyushkin, and N. G. Stefanis, Phys. Rev. D 62 (2000) 113001.

Бакулев А.П., Михайлов С.В., Стефанис Н.Г.   E2-2001-60

Амплитуда распределения π-мезона в КХД
и новые экспериментальные данные

В формализме правил сумм КХД с нелокальными конденсатами переоцениваются моменты амплитуды распределения (АР) π-мезона твиста-2 и отвечающие им доверительные интервалы. В результате на плоскости гегенбауэровских коэффициентов (a_2, a_4) построена область допустимых значений для АР пиона. Подчеркивается, что модели типа Черняка–Житницкого так же, как и асимптотическая АР, не входят в эту область. Показано, что определенная область допустимых значений коэффициентов a_2 и a_4 сильно перекрывается с областью, извлеченной из экспериментальных данных CLEO Шмеддингом и Яковлевым (2000), по формфактору перехода $\gamma^*\gamma \to \pi$ в рамках пертурбативной КХД и находится вблизи от АР, полученной (нами) из первого эксперимента по прямому измерению импульсного распределения валентных кварков в пионе (сотрудничество E-791 Лаборатории им. Э.Ферми). Кратко обсуждаются результаты других недавних работ (инстантоны и решетка).

Bakulev A.P., Mikhailov S.V., Stefanis N.G.   E2-2001-60

QCD-Based Pion Distribution Amplitudes Confronting Experimental Data

We use QCD sum rules with nonlocal condensates to recalculate more accurately the moments and their confidence intervals of the twist-2 pion distribution amplitude including radiative corrections. We are thus able to construct an admissible set of pion distribution amplitudes which define a reliability region in the a_2, a_4 plane of the Gegenbauer polynomial expansion coefficients. We emphasize that models like that of Chernyak and Zhitnitsky, as well as the asymptotic solution, are excluded from this set. We show that the determined a_2, a_4 region strongly overlaps with that extracted from the CLEO data by Schmedding and Yakovlev and that this region is also not far from the results of the first direct measurement of the pion valence quark momentum distribution by the Fermilab E791 collaboration. Comparisons with recent lattice calculations and instanton-based models are briefly discussed.

Макет Т.Е.Попеко